

## Accepted Manuscript

Gas solubility and rheological behavior study of betaine and alanine based natural deep eutectic solvents (NADES)

Tausif Altamash, Mustafa S. Nasser, Yousef Elhamarnah, Musaab Magzoub, Ruh Ullah, Hazim Qiblawey, Santiago Aparicio, Mert Atilhan



PII: S0167-7322(17)36134-2  
DOI: doi:[10.1016/j.molliq.2018.02.049](https://doi.org/10.1016/j.molliq.2018.02.049)  
Reference: MOLLIQ 8691  
To appear in: *Journal of Molecular Liquids*  
Received date: 22 December 2017  
Accepted date: 6 February 2018

Please cite this article as: Tausif Altamash, Mustafa S. Nasser, Yousef Elhamarnah, Musaab Magzoub, Ruh Ullah, Hazim Qiblawey, Santiago Aparicio, Mert Atilhan , Gas solubility and rheological behavior study of betaine and alanine based natural deep eutectic solvents (NADES). The address for the corresponding author was captured as affiliation for all authors. Please check if appropriate. Molliq(2017), doi:[10.1016/j.molliq.2018.02.049](https://doi.org/10.1016/j.molliq.2018.02.049)

This is a PDF file of an unedited manuscript that has been accepted for publication. As a service to our customers we are providing this early version of the manuscript. The manuscript will undergo copyediting, typesetting, and review of the resulting proof before it is published in its final form. Please note that during the production process errors may be discovered which could affect the content, and all legal disclaimers that apply to the journal pertain.

**Gas Solubility and Rheological Behavior Study of Betaine and Alanine Based  
Natural Deep Eutectic Solvents (NADES)**

Tausif Altamash<sup>1</sup>, Mustafa S. Nasser<sup>2\*</sup>, Yousef Elhamarnah<sup>2</sup>, Musaab Magzoub<sup>2</sup>, Ruh Ullah<sup>3</sup>, Hazim Qiblawey<sup>1</sup>, Santiago Aparicio<sup>4\*</sup> and Mert Atilhan<sup>5,6\*</sup>

<sup>1</sup>Department of Chemical Engineering, Qatar University, Doha, Qatar

<sup>2</sup>Gas Processing Center, Qatar University, Doha, Qatar

<sup>3</sup>National Institute for Materials Science (NIMS), Japan

<sup>4</sup>Department of Chemistry, University of Burgos, Burgos, Spain

<sup>5</sup>Department of Chemical Engineering, Texas A&M University at Qatar, Doha, Qatar

<sup>6</sup>Gas and Fuels Research Center, Texas A&M University, College Station, TX, USA

\**Corresponding Authors:* Prof. Mert Atilhan mert.atilhan@tamu.edu, Prof. Santiago Aparicio sapar@ubu.es and Prof. Mustafa Saleh m.nasser@qu.edu.qa

**ABSTRACT**

Natural deep eutectic solvent (NADES) produced herein this work by mixing betaine and alanine with lactic acid and malic acid with 1:1 molar mixing ratios. Thermophysical properties including water content, thermal stability, density and gas solubility of CO<sub>2</sub> and N<sub>2</sub> were experimented at different isotherms for wide pressures range up to 50 bars. Moreover, detailed rheological experiments were conducted on the studied materials to obtain viscosity and deduce the dynamic flow behavior. A pressure driven physisorption mechanism was observed for the studied systems. Betaine based NADES materials showed superior carbon dioxide and nitrogen solubility when they are mixed with lactic acid. On the other hand, the rheological experimental results show shear-thinning effect in which the  $\eta$  is decreasing with shear rate at all temperatures. Low viscosity profiles NADES assure the less mass transfer resistance for lactic acid based NADES systems and it also confirmed that the high CO<sub>2</sub> and N<sub>2</sub> solubility for lactic acid based NADES samples.

**Keywords:** Deep Eutectic Solvents, Natural Products, Gas Solubility, Rheology

ACCEPTED MANUSCRIPT

## 1. INTRODUCTION

Increasing anthropogenic carbon dioxide (CO<sub>2</sub>) levels in the atmosphere and in the oceans have become one of the grand challenge of the mankind in recent years[1]. Unprecedented amounts of CO<sub>2</sub> in the atmosphere are mainly due to the uncontrolled usage of fossil based fuels and its consequent emissions of greenhouse gases to the atmosphere[2]; and such emissions are mostly come from the power generation plants and other chemical processing processes[3]. Thus; these industries are more aggressive means of gas sorption technologies in order to reduce the toxic gaseous emissions and meet the global agreements for low carbon emissions. An amine-based absorption process has been utilized in chemical process industries since the 1950s due to its high sorption capability, selectivity and stable nature. Moreover, most of the existing chemical processes utilized amine based sorption systems as current state of the art for CO<sub>2</sub> capture and mitigation[4]. However, due to problems such as high corrosion[5, 6], solvent degradation[7], and high regeneration costs[8], amine based CO<sub>2</sub> capture processes lead to large increases in operating costs of the processes and eventually lead to large increase in the cost of electricity production. Although there are ongoing efforts for improving the current state-of-the-art sorption systems by retrofitting the already established CO<sub>2</sub> capture processes via the application of advanced process systems and engineering tools (e.g. heat and mass integration)[9], above mentioned drawbacks for the amine systems urge chemical industries to seek for sustainable solutions both economically and technologically in order to manage toxic emissions in the last few decades. Ionic liquids (ILs), molten salts consist of cation and anion and typically exist in liquid state at room temperatures, have been seriously considered for such purpose since their nature that allows to achieve tailor made thermophysical properties. Hence, some ILs (e.g. imidazolium based ILs) have gained attention in the recent years due to since they have shown abilities to provide acceptable level of CO<sub>2</sub> solubilization and adoptability at wide process conditions that includes both pre- and post- combustion CO<sub>2</sub> removal[10]. Moreover, ILs have been used in wide range of other applications such as chemical or enzymatic reactions[10-12], biocatalytic process[13], extraction solvent[13, 14], electrochemical applications[15], olefin paraffin separation[16] and biomedical applications[17]. Despite its advantages, due to limited biodegradability, poor

biocompatibility, high viscosity[18] and high production cost at bulk quantities[19, 20] other alternatives have been on the rise.

Deep Eutectic Solvents (DES) is one of the alternatives to ILs that has the similar features of ILs. DES are obtained with the mixture of two or more components with a melting point lower than either of its individual constituents[19, 21]. They are typically obtained by mixing a quaternary ammonium halide salt, which act as a hydrogen bond acceptor (HBA), with a hydrogen bond donor (HBD) molecule, which forms a complex with the halide. Combination of HBD and HBA forms the solvent that is called DES, and this combination leads to a significant depression in the freezing point[22, 23].

Due to the availability of many HBA and HBD, there are abundant amount of possible DES could be foreseen. The advantage of working DES is the capability of the materials and preparation process that allows us to adjust the thermophysical properties of the DES by choosing the desired combination of the DES formers. DES systems can be tailor made and used for applications such as organic reactions, extractions and synthesis[24-28], electrochemistry[29-31], enzymatic reactions[32-35], biotransformations[36], biodiesel production[37], polymer synthesis and applications[38], and potential transdermal drug delivery applications[39]. When the HBD and HBA fomers of the DES are produced from naturally available chemicals, then the new solvent is called as natural deep eutectic solvents (NADES). Typical examples of NADES include eutectic mixtures of amino acids and/or sugars with organic acids[40, 41]. Main advantage of NADES over DES (also ILs) is that the ability to prepare NADES at very low toxicity levels. Some recent studies hypothesizes that there are some examples of NADES in living organisms and it is believed to lead the biosynthesis of poorly water-soluble metabolites and macromolecules in the aqueous environments[24, 41]. NADES are considered as viable alternatives, since they have very low vapor pressure that prevents the solvent losses[42]. Moreover they are much cheaper to produce when compared with exotic solvents as well as ILs, they are biodegradable and biocompatible, which makes their disposal straightforward and inexpensive[21, 43].

In order either DES or NADES to be considered as an alternative gas sweetening solvent in larger scales by the regulatory authorities, thermophysical properties that include gas solubility performance as well as detailed rheological behavior must be

investigated for various potential systems. Thus, the main purpose of this work is to contribute to such needs by focusing on selected NADES systems and study their thermophysical properties at various isotherms at wide pressure conditions up to 50 bars. In a previous work, choline chloride based NADES systems, which were prepared by mixing malic acid, lactic acid, citric acid and fructose[44]. In this work, we have selected naturally available amino acids, betaine and alanine, and studied their mixtures with lactic acid and malic acid.

## 2. MATERIAL AND METHODS

Alanine (Al) with  $\geq 98\%$  purity (CAS Number 56-41-7) with melting point of 258 °C, betaine (Be) with  $\geq 98\%$  purity (CAS Number 107-43-7) with melting point of 310 °C, DL-malic acid (Ma) with 99% purity (CAS Number 6915-15-7), lactic acid (La) with 85% purity (CAS Number 50-21-5) were purchased from Sigma Aldrich. Gases that were used ( $\text{CO}_2$  and  $\text{N}_2$ ) with purities of  $\geq 99.99\%$  were obtained from Buzware Scientific Technical Gases, Qatar. In order to form NADES samples, (Al) and (Be) were mixed with (La) and (Ma) with 1 to 1 (1:1) molar mixing ratios by following vigorous stirring of the mixture until a clear-homogenous in a glove box in which atmosphere and humidity were controlled. All of the prepared NADES samples were observed to be liquid state at room temperature. The details of the chemical structures and physical properties of the studied NADES mixtures are given in Table 1 and the pictures of the studied NADES samples are given in Figure 1. Prepared samples were kept at dried environment and at room temperature prior to characterization, gas solubility and rheology experiments. Considering the fact that an easy synthesis process was followed in which no solvent was added and yet no additional steps were included for purification, only heat was supplied in order to keep samples' liquid state during their preparation.

**Table 1.** Properties of studied NADES samples in this work.

**Figure 1.** Picture of the studied NADES samples in this work.

In order to observe the hygroscopic behavior of the NADESs, water content was obtained by using Karl Fischer moisture titrator (Model C20) and values are included in Table 1. Density experiments were conducted at various isotherms via Anton Paar DMA 4500M vibrating tube densimeter. Water was used for the densimeter calibration, and

reference density values for water were obtained from the fundamental equation of state by Wagner and Pruss (uncertainty lower than  $\pm 0.003$  % in the full pressure and temperature ranges)[45]. Moreover, further calibration was conducted by using dimethyl sulfoxide (DMSO) at various isotherms and experimental results were compared with literature values. Further details on the calibration of the vibrating tube apparatus can be obtained elsewhere[46]. The uncertainty temperature and the pressure measurements in densitometer is  $\pm 0.05$  K and 0.005 MPa. Calculated relative uncertainty for the experimental density values, which also considers the samples impurities was estimated to be as 0.3 % ( $\pm 0.00005$  g m<sup>-3</sup>). Thermal gravimetric analysis (TGA) were performed on the studied NADESs for their thermal stability, determination of the decomposition temperature and their onset temperatures by using PerkinElmer Pyris 6 TGA apparatus. Samples were heated from 303 to 773 K with the temperature increase rate of 5 K min<sup>-1</sup> under dried atmosphere using N<sub>2</sub> gas to obtain the weight loss curve. Moreover, for material characterization Fourier-transform infrared (FTIR) spectrums of the materials were taken via Bruker® Vertex 80 spectrometer. For studied NADES samples IR spectrums between 4000 cm<sup>-1</sup> to 400 cm<sup>-1</sup> were investigated and related peaks were analyzed accordingly.

Rubotherm magnetic suspension sorption apparatus (MSA), operates by using Archimedes' buoyancy principle, was used for high-pressure gas absorption-desorption experiments. A detailed explanation of its working principles, data correlation, magnetic suspension force transmission error correction and related calibration were previously studied and published elsewhere by using wide range of adsorbents and absorbents[11-13, 41, 47, 48].

The apparatus has in-situ density measurement capability (with 4 kg m<sup>-3</sup> uncertainty) that enables direct gravimetric measurements during the sorption experiments. Pressure transducers (Paroscientific, USA) works from vacuum up to 350 bar with an uncertainty of 0.01% of the full scale ( $u(p) \approx 0.035$  bar), whereas temperature sensor (Minco PRT, USA) has a measurement accuracy of  $\pm 0.5$  K ( $u(T) = 0.05$  K). Fully automated sorption apparatus first measures the vacuum point and then moves to pressure points as determined by the operator; stays at each pressure point until the equilibrium is reached (typically 45 to 60 min) and then the system goes to the next pressure point. Apparatus is

operated to measure low pressure towards high pressure (adsorption) and then from high pressure to low pressure (desorption) including the end-of-sorption-cycle vacuum point measurement, in order to check whether chemisorption takes place during the sorption cycle. Vacuum was applied for each sample for at least 10 hours and the sorption cycle that is explained above was repeated for the same NADES sample (unchanged sample in the measurement bucket) each for experimental isotherms at 298.15 K, 308.15 K, 318.15 K and 328.15 K for both CO<sub>2</sub> and N<sub>2</sub>. Each studied NADES samples were tested in cyclic measurement routines for at least 3 cycles, in order to observe whether there is degradation in activity of the studied specimens.

The rheological measurements were carried using a strain instrument (Anton Paar Rheometer Model MCR 302). 50 mm diameter cone and plate measurement geometry was used with a gap of 0.104 mm. Samples were allowed to rest for 5 minute equilibration time before the flow test was started. Controlled shear stress tests were conducted by varying the shear rate from 0.01-1000 s<sup>-1</sup>. To conduct the strain sweep tests within, linear the viscoelastic range (LVR), a constant frequency is selected and the strain is varied to determine the LVR. Both the storage modulus ( $G'$ ) and loss modulus ( $G''$ ) are independent of strain. The applied frequency range was between (0.1 – 100 rad/s) at constant strain of 0.1 to determine the storage modulus ( $G'$ ), loss modulus ( $G''$ ), complex viscosity ( $\eta^*$ ). The  $G'$  and  $G''$  were determined by extrapolating the low applied frequency to the zero coordinate. All the rheological measurements in this paper were carried out in triplicate and the average values are used. The experimental results obtained in this study were reproducible with error less than 5%.

### 3. RESULTS AND DISCUSSIONS

#### 3.1 Characterization

Water content reported in Table 1 is in the range of 0.7 to 5.4 wt %. The studied NADES are highly hydrophylic compounds, and thus samples with reasonable water content were used along this work. Moreover, in a recent publication water content value for similar structures were reported to be in between 8140 ppm to 69380 ppm (~ 0.8 to 7.0 wt %)[49], which is similar to our reported values in this work. The use of totally dried samples (by extensive vacuum drying) would lead to physicochemical data for



ultrapure NADES, but these samples would not represent industrial conditions in which NADES would not be handled under inert atmosphere due to technical and economical reasons. Therefore, the reported physicochemical properties for the samples with the reported water content would represent NADES under realistic industrial conditions. Density experiments were conducted via automated vibrating tube densimeter at atmospheric conditions at various isotherms up to 90 °C. Experimental density plots are provided in Figure 2 and density values are provided in Table S1 (Electronic Supporting Information – ESI). Density measurements for Be:Ma sample conducted between 45 °C to 65 °C, since the melting point temperature for Be:Ma NADES sample was found to be as  $\sim 45$  °C ( $318.15 \pm 1$  K). At room temperature and atmospheric conditions, density values for the studied NADES samples were found to be as 1.207, 1.415 and 1.282 g.cm<sup>-3</sup> for Be:La, Al:Ma and Al:La respectively. Linear monotonically decreasing density profiles (with  $R^2 \sim 0.99$ ) are observed with the increasing temperature in Figure 2 for the studied NADES samples. Amongst the other studied samples, Al:Ma has shown higher density values. Al:La density profile is almost similar with the density profile of the previously studied choline chloride:malic acid (ChCl:Ma) NADES sample. Moreover, Al:Ma and Be:Ma density profiles also observed to be very similar to each other in Figure 2. According to experimental density values, studied NADES systems can be ranked as Al:Ma > Be:Ma > Al:La > Be:La. Thermal expansion coefficients of the NADESs were calculated from the density vs temperature data as 0.000570, 0.000521, 0.000570, 0.000538 1/°C for Al:Ma, Be:Ma, Al:La, Be:La respectively.

**Figure 2.** Density values of Be:La, Be:Ma, Al:La, Al:Ma and comparison with previously studied NADES and DES systems (Paa=Phynlacetic acid, Laa=levulinic acid, ChCl=choline chloride, Fr=fructose).

Water content of the studied samples was also calculated via Karl/Fisher method as explained in previous section. According to presented water content values in Table 1, studied NADES samples can be ranked for their moisture contents as Al:Ma > Al:La > Be:Ma > Be:La. Particularly Al containing Al:Ma and Al:La samples have relatively higher water content, 5.4% and 4.4% (saturation values) respectively. This could be explained as, despite hydrophobic behavior of both Al and Be, since Al has an amine

functionality it makes it absorb more water when compared with other hydrophobic aminoacids such as glycine when compared with Be, histidine and glycine[50]. When density profiles and water content rankings are compared, it can be observed that despite lower viscosity of water in comparison to constituents of NADES samples, water could not dominate the system and HBD showed superior effect in the determination of the final density values. In Figure 2, NADES density values and density values for some DES samples, which were obtained via the mixture of ChCl with non-natural organic acids, levulinic acid (Laa)[51] and phenyl acetic acid (Paa)[46], were compared. Density values of NADES that were obtained from the naturally existing HBD have yielded higher density values. On the other hand, when the density values were compared with the other previously published other NADES samples[44], Al:Ma has showed a distinctly higher density profile than the others, as can be seen in Figure 2.

TGA were performed on the studied NADESs for their thermal stability, determination of the decomposition temperature ( $T_d$ ) and their onset temperatures ( $T_{onset}$ ), as given in Figure 3 in terms percentage weight loss with respect to temperature from in the range of 298 K to 800 K. The overall observation on the thermal stability of the studied NADES shows that their suitability for the implementation of Al and Be based NADESs can be implemented in industrial application at wide process conditions including high temperature operations that includes both pre- and post- combustion CO<sub>2</sub> capture processes. Al:La, Be:Ma and Be:La NADES samples have showed very similar decomposition trends and they followed a single step degradation with approximated  $T_d$  values of around ~220 K. Whereas, a two step degradation is observed for Al:Ma with the first step  $T_d$  of ~220 K and second step  $T_d$  of ~320 K. This distinct behavior can be explained due to its 5.4% water content.

**Figure 3.** TGA analysis for Be:La, Be:Ma, Al:LA and Al:MA NADES systems.

Fourier-transform infrared (FTIR) spectrums of the materials were taken via Bruker® Vertex 80 spectrometer and FTIR plots that indicates the certain characteristic peaks are provided in Figure 4. Typically, amino acids show large number of hydrogen bonding as can be observed by the existence of broad bands mostly within the region of 3000-2000 cm<sup>-1</sup> in their spectra, which makes it challenging to distinguish between the C-H and N-H bands. Final NADES structures shall exhibit both certain characteristic peaks

for both amino acid and organic acids. Figure 4a (Be:Ma) has characteristic peaks at 1716 (C=O), 2519 (O-H) and 1324 (C-O)  $\text{cm}^{-1}$  that corresponds to Ma; and Figure 4b (Be:La) displays similar characteristic peaks for La at 1724 (C=O), 2503 (O-H) and 1221 (C-O)  $\text{cm}^{-1}$ . For both Be based NADES samples, peaks that corresponds to Be were observed to be as 1716 (carbonyl) and 1609 (COO)  $\text{cm}^{-1}$  for Be:Ma; 1724 (carbonyl) and 1629 (COO)  $\text{cm}^{-1}$  for Be:La. On the other hand, alanine has broad bands characteristics typically observed at 2300 and 3050  $\text{cm}^{-1}$ . This broad bands were observed for both Al:La and Al:Ma in Figure 4c and Figure 4d respectively. Moreover, a broad N-H bending mode was also observed around 2130  $\text{cm}^{-1}$  for both Al based NADES samples. Other than these, for Al:Ma peaks at 640, 896 and 1040  $\text{cm}^{-1}$ , and for Al:La peaks at 656, 970 and 1036  $\text{cm}^{-1}$  were recorded for COO,  $\text{NH}_2$  and  $\text{CH}_3$  characteristics that corresponds to Al structure. Last but not least, for Al:Ma 1708, 2944, 1210  $\text{cm}^{-1}$  and for Al:La 1720, 2910, 1295  $\text{cm}^{-1}$  that corresponds to C=O, O-H and C-O stretch respectively.

**Figure 4.** FTIR analysis for Be:La, Be:Ma, Al:LA and Al:MA NADES systems.

### 3.2 Gas Solubility

Gas solubility ( $\text{CO}_2$  and  $\text{N}_2$ ) experiments for Be:La, Be:Ma, Al:LA and Al:MA NADES systems were performed at 298.15K, 308.15 K, 318.15 K and 328.15 K and pressures up to 50 bars by using gravimetric method. Adsorption-desorption cycles for each NADES were studied in order to observe hysteresis and physisorption behavior. For each sample, 20 pressure points were studied at each isotherm (12 absorption, 8 desorption). Buoyancy corrections on the sorption data conducted via using in-situ density measuring capability of the MSA. Moreover, other external conditions such as humidity, ambient pressure and temperature were considered by the apparatus for zero-point corrections of the measurement routine in order to achieve higher reliability solubility data. Numerical data for the  $\text{CO}_2$  and  $\text{N}_2$  solubility for all studied NADESs are provided Table S2-S5. Solubility plots for Be:La, Be:Ma, Al:La and Al:Ma are provided in Figures 5, 6, 7 and 8 respectively.

**Figure 5.** Gas sorption in Be:La NADES system at different isotherms; (a)  $\text{CO}_2$  (b)  $\text{N}_2$  (closed symbols are absorption and open symbols are desorption)

**Figure 6.** Gas sorption in Be:Ma NADES system at different isotherms; (a) CO<sub>2</sub> (b) N<sub>2</sub> (closed symbols are absorption and open symbols are desorption)

Solubility trends have showed solubility of both CO<sub>2</sub> and N<sub>2</sub> is increased with increasing pressure and decreasing temperature. Solubility decrease with the increase of temperature can be explained with the kinetic energy of the gas molecules; as it is increased with the increasing temperature, gas molecules break the intermolecular bonds that are formed within the solute and gain higher inclination to escape from the solution. No hysteresis was observed during the solubility measurements, which eliminates the potential swelling effect of the liquids under such pressure conditions. Experimented solubility trends fit to absorption profile type III[52, 53]. However, solubility figures show that there is still an increasing trend in the solubility plot, which means there is still a potential for higher solubility in studied NADESs. Nevertheless, going beyond 50 bars would be practically challenging from both processing and economic reasons in large-scale applications, considering the viscosity limitations (explained in section 3.3). Solubility tests were performed at least 3 times on each of the NADESs and no significant change was observed on the performance of the gas solubility. At each solubility measurement, end-of-the-experiment vacuum measurements yielded the same mass reading as at the beginning of the experimental routine; which means no residual CO<sub>2</sub> (or N<sub>2</sub>) remained in the sample at the end of the run. Thus, chemisorption is eliminated and all the presented solubility data is based on the physisorption behavior. When no-hysteresis and physisorption behaviors are considered, presented NADESs are suitable for pressure swing absorption (PSA) method in large-scale application.

**Figure 7.** Gas sorption in Al:La NADES system at different isotherms; (a) CO<sub>2</sub> (b) N<sub>2</sub> (closed symbols are absorption and open symbols are desorption)

**Figure 8.** Gas sorption in Al:Ma NADES system at different isotherms; (a) CO<sub>2</sub> (b) N<sub>2</sub> (closed symbols are absorption and open symbols are desorption)

Comparison of the maximum gas solubility data can be made at based on the minimum of 318 K isotherm data, since Be:Ma were observed to be at liquid state only at ~318 K. Experiments resulted 3.593, 3.489, 3.332, 1.950 mmol of CO<sub>2</sub>/g NADES and 5.644, 2.663, 5.550, 3.065 mmol of N<sub>2</sub>/g NADES for Be:La, Be:Ma, Al:La and Al:Ma respectively. When both highest CO<sub>2</sub> and N<sub>2</sub> sorption performance is considered, Be:La

has the highest solubility for both cases. Be:La, Al:La and Al:Ma samples had higher solubility performance for  $N_2$  than they have for  $CO_2$ . Be based NADES samples showed higher  $CO_2$  solubility than that of Al based NADES samples. When selectivity of  $N_2:CO_2$  is considered at 318 K values of 1.6, 1.7, 1.6 were obtained for Be:La, Al:La, Al:Ma respectively. For Be:Ma  $CO_2:N_2$  selectivity was calculated as 1.3. When HBD effects are considered, La has showed an interesting two folds superior absorption performance with respect to Ma in the case of they were mixed with either HBA. As an overall observation based on the selectivity values,  $N_2:CO_2$  selectivity decreased with increasing temperature. Selectivity values are not observed to be high, therefore based on those values there is no significant lead on either of the gases.

**Figure 9.** Maximum gas sorption in studied NADES systems.

It is evident that Be played a dominant role in the  $CO_2$  sorption performance and it can be explained with the direct  $COO-CO_2$  interaction. Water ( $H_2O$ ) content of the studied NADES systems also plays a role on the  $CO_2$  sorption.  $H_2O$  leads to  $OH-H_2O-CO_2$  interaction mechanism in the solvent when exists, and it can be used to fine tune or control the sorption performance as well as the viscosity of the solvent. When studied NADESs are considered for this work, as mention previously, Be dominates the entire  $CO_2$  affinity mechanism and even goes beyond the effect of natural carboxylic acid that comes from the HBD and leads the sorption mechanism entirely. Speaking of the HBD, it seems like La seems to improve the sorption performance both for  $CO_2$  and  $N_2$  when combined with the HBA (Be and Al).

### 3.3 Rheological behavior

#### 3.3.1 Flow Behaviour

An example of a dynamic strain sweep test to determine the LVR is provided in Figure 10.

**Figure 10.** Dynamic Strain Sweep used to derive the linear viscoelastic range for Be: LA and Al:La samples at a constant frequency of 5 rad/sec and at 25°C.

The rheological behavior of the studied NADES systems showed the shear-thinning effect in which the NADES viscosities decreased with shear rate at all temperatures. This can be attributed to the structural breakdown caused by structure

thermal expansion and shearing effect [54-58]. Figure 11 shows apparent viscosity as a function of temperature for different NADES systems at low shear rate of  $1 \text{ s}^{-1}$  as sheared for 5 minutes. The NADES viscosities vary greatly with the nature of the constituting components of the hydrogen bond donor (i.e. (La) and (Ma)) and hydrogen bond acceptor (i.e (Be) and (Al) and the temperature. It was found that, at room temperature, the NADES samples contains malic acid in the case of Be:Ma and Al:Ma were not were not liquid and they behaved like semi-solid materials showing very high viscosity (over  $4.8 \times 10^6 \text{ mPa}\cdot\text{s}$  for Be:Ma and  $5.0 \times 10^5 \text{ mPa}\cdot\text{s}$  for Al:Ma). Once the melting point of both samples ( $50 \text{ }^\circ\text{C}$ ) was exceeded, the mixture behaves gel-like material and viscosities drops significantly. On the other hand, the NADES samples contains lactic acid in the case of Be:La and Al:La were liquid at room temperature showing lower viscosities ( $1.8 \times 10^4 \text{ mPa}\cdot\text{s}$  for Be:La and  $2.2 \times 10^4 \text{ mPa}\cdot\text{s}$  for Al:La). This leads to the conclusion that the malic acid based NADESs have a much higher viscosity at low temperatures than other lactic based NADESs investigated here. Low viscous NADES liquids are generally more desirable as it will be easier to apply them as solvent for many industrial applications such as  $\text{CO}_2$  capture or as a catalyst. High viscosity for NADES is not recommended as this will increase the energy cost for pumping and handling of the NADES[44, 46, 59].

**Figure 11.** Effect of heating on the apparent viscosity (at low shear rate of  $1 \text{ s}^{-1}$ ) for studied NADES systems

In many industrial processes, some of these high viscous NADES required preheating before processing and need more pumping energy as well. As there are no available models to predict the viscosity of the NADESs, using rheological model such as Bingham model to fit the experimental measurements could be beneficial in assessing their applicability as well as building predictive models. Bingham plastic model can be used to describe the viscosity function and to estimate the Bingham yield stress ( $\tau_B$ ) values[60-62]. The magnitude of  $\tau_B$  is a useful parameter that can be used as indicative of the amount of minimum stress required disrupting the networked structure in order to initiate the flow which is normally correlated to the pumping energy required to initiate flow, any stress below  $\tau_B$  for the mixture means that the mixture behaves as a rigid solid. In this study, Bingham plastic model well described the flow behavior of the four

NADES systems tested and the variation of yield stress as a function of the temperature for the studied NADES systems are illustrated in Figure 12.

**Figure 12.** The variation of yield stress as a function of the temperature for the studied NADES systems

The results showed that the yield stresses of all NADESs decreased with increasing temperature as expected for the shear thinning materials. The differences in the yield stress values are mainly due to the changes in the interaction forces between the hydrogen bond donor and hydrogen acceptor of the NADES and the molecular weight[44, 46]. The variations of the yield stress values as a function of temperature is similar to the viscosity data (see Fig. 10), it was found that the lactic acid based NADES systems (Be:La and Al:La) have lower yield stress values than malic based NADES systems (Be:Ma and Al:Ma). At room temperature, the ratio of  $\tau_B(Al:Ma): \tau_B(Al:La)$  is around 18 and  $\tau_B(Be:Ma): \tau_B(Be:La)$  is around 13. In addition, at high temperature, the La NADES yield stresses were less sensitive to the temperature as they remain almost constant. Lower yield stress values are of good advantage for industrial applications such as CO<sub>2</sub> capture.

### 3.3.2 Viscoelastic Behavior

The interaction forces between the hydrogen bond donor and hydrogen acceptor of the NADES can be further investigated using the oscillatory viscoelastic behaviour of the NADES by calculating the storage modulus ( $G'$ ), loss modulus ( $G''$ ) and complex viscosity ( $\eta^*$ ). The oscillatory rather than steady shear measurements were normally used to avoid any damage of the material formed networks [63]. The  $\eta^*$  is correlated to  $G'$  and  $G''$  through the complex dynamic modulus ( $G^*$ )[63-66] using eq. 1 and 2:

$$G^* = G' + iG'' \quad (1)$$

$$\eta^* = \frac{G^*}{\omega} \quad (2)$$

where  $\omega$  is the angular frequency. The variations of  $G'$  and  $G''$  as a function of angular frequency at different temperatures were measured for all NADES systems. The frequency dependence of  $G'$  and  $G''$  at 25 °C is shown in Fig. 12. The results confirm that the four tested NADES,  $G''$  values are higher than  $G'$  over the whole applied frequency

range. This indicates that all solvents are more like viscous liquids and not like solid materials. The greater difference in the values of  $G''$  and  $G'$  (e.g.  $G'' \gg G'$ ) indicating presence of more flow components in the gels making the gels behave like viscous liquid and as the  $G' \rightarrow 0$  the material behave as ideal viscous flow behavior. At frequency of 100 rad/s and at room temperature, the NADES samples contains malic acid showed higher  $G'$  ( $7.2 \times 10^7$  mPa for Be:Ma and  $3.3 \times 10^7$  mPa for Al:Ma) comparing to the lactic acid based NADES ( $2.3 \times 10^5$  mPa for Al:La and  $1.1 \times 10^5$  mPa for Be:La). The summarized values of  $G'$ ,  $G''$  and  $\eta^*$  as a function of temperature and at frequency of 1 rad/s for the four NADES systems are shown in Figure 13. The values of  $G'$ ,  $G''$ , and  $\eta^*$  decreased as the temperature increased for all NADES systems as expected for the shear thinning materials and this is mainly due to the changes in the interaction forces between the hydrogen bond donor and hydrogen acceptor of the NADES and due to the thermal expansion. Also the variation of dynamic complex viscosity ( $\eta^*$ ) with temperature is in good agreement with shear apparent viscosity ( $\eta$ ) shown in figure 10.

**Figure 13.** The variation of yield stress as a function of the angular frequency for the studied NADES systems

**Figure 14.** The variation of (a) Storage modulus ( $G'$ ), (b) loss modulus ( $G''$ ) and (c) complex viscosity ( $\eta^*$ ) for the NADES systems with temperature at constant frequency of 1 rad/s

Considering the shear and dynamic frequency sweep rheological measurements one can conclude that the flow behaviour of lactic acid based (Be:La and Al:La) NADES systems are most suitable for the applications such as  $\text{CO}_2$  capture comparing to malic acid based (Be:Ma and Al:Ma) NADES systems where preheating or pumping are required. This observation coincides with the experimental gas solubility data as well. Therefore, the effect of heating (Ramp up) and cooling (Ramp down) on the apparent viscosity for the same samples of Be:La and Al:La NADES systems are further investigated and presented in Figure 15. Increasing the temperature from 25-120 °C primarily affected the viscosity properties of both systems (as shown before). Reversibility (cooling) was also investigated by decreasing the temperature from 120 to 25 °C and the rheological results showed comparable profiles for the “ramp up” and reversible “ramp down” tests. This suggested that the lactic acid based NADES has



maintained its structural characteristics even after the temperature had increased to 120°C. The thermal stability of this material is of great advantage in many chemical processes including CO<sub>2</sub> capture.

**Figure 15.** Effect of heating (Ramp up) and cooling (Ramp down) on the apparent viscosity (at low shear rate of 1 s<sup>-1</sup>) for (a) Be:La and (b) Al:La NADES systems

#### 4. CONCLUSIONS

In this work, natural occurring HBD and HBA were mixed to form natural deep eutectic solvents (NADES). Be, Al, La and Ma were used with 1:1 mixing ratio to form Be:La, Be:Ma, Al:La and Al:Ma NADESs. A detailed characterization that includes density, water content, thermal gravimetric analysis (TGA), Fourier-transform infrared (FTIR), gas solubility of CO<sub>2</sub> and N<sub>2</sub> at various isotherms and pressures up to 50 bars were investigated. Moreover, rheological behavior of the studied NADESs was investigated in order to describe the dynamic flow behavior of the samples. According to gas solubility experimental data, best performing absorbent for both CO<sub>2</sub> (3.59 mmol/g) and N<sub>2</sub> (5.64 mmol/g) is Be:La. When the selectivity of the materials is considered (based on the single gas sorption data), there is no significant superiority one on another amongst the studied systems; however in terms of the single gas absorption performance studied NADESs can be considered as competitive with respect to current benchmark liquid absorbents at studied pressure and temperature ranges. La has showed an interesting two folds superior absorption performance with respect to Ma in the case of they were mixed with either HBA. With respect to rheology experiments, at high temperature La NADESs yield stresses were less sensitive to the temperature as they remain almost constant, which is an advantage for industrial applications such as CO<sub>2</sub> capture. On the other hand, considering the shear and dynamic frequency sweep rheological measurements one can conclude that the flow behavior of lactic acid based (Be:La and Al:La) NADES systems are most suitable for the applications such as CO<sub>2</sub> capture comparing to malic acid based (Be:Ma and Al:Ma) NADES systems where preheating or pumping are required. This observation coincides with the experimental gas solubility data as well.

## SUPPORTING INFORMATION

Electronic supporting information (ESI) document includes numerical experimental data on density measurements and gas solubility measurements (for both CO<sub>2</sub> and N<sub>2</sub>) for the studied NADESs.

## ACKNOWLEDGEMENTS

This work was made possible by NPRP grant # 6-330-2-140 from the Qatar National Research Fund (a member of Qatar Foundation) and by Ministerio de Economía y Competitividad (Spain, project CTQ2013-40476-R).

## CITED REFERENCES

- [1] R. Monastersky, *Nature* 2013 497 (2013) 13.
- [2] N. Du, H.B. Park, G.P. Robertson, M.M. Dal-Cin, T. Visser, L. Scoles, M.D. Guiver, *Nat Mater* 10 (2011) 372.
- [3] H.A. Patel, S. Hyun Je, J. Park, D.P. Chen, Y. Jung, C.T. Yavuz, A. Coskun, 4 (2013) 1357.
- [4] M. Wang, A. Lawal, P. Stephenson, J. Sidders, C. Ramshaw, *Chem. Eng. Res. Des.* 89 (2011) 1609.
- [5] J. Kittel, R. Idem, D. Gelowitz, P. Tontiwachwuthikul, G. Parrain, A. Bonneau, *Energy Procedia* 1 (2009) 791.
- [6] A. Rafat, M. Atilhan, R. Kahraman, *Industrial & Engineering Chemistry Research* 55 (2016) 446.
- [7] S. Martin, H. Lepaumier, D. Picq, J. Kittel, T. de Bruin, A. Faraj, P.-L. Carrette, *Industrial & Engineering Chemistry Research* 51 (2012) 6283.
- [8] M. Vaccarelli, R. Carapellucci, L. Giordano, *Energy Procedia* 45 (2014) 1165.
- [9] S.J. Higgins, Y.A. Liu, *Industrial & Engineering Chemistry Research* 54 (2015) 2526.
- [10] F. Karadas, M. Atilhan, S. Aparicio, *Energy & Fuels* 24 (2010) 5817.
- [11] A.E. Visser, R.P. Swatloski, R.D. Rogers, *Green Chemistry* 2 (2000) 1.
- [12] T. Welton, *Chem. Rev.* 99 (1999) 2071.

- [13] A. Paiva, R. Craveiro, I. Aroso, M. Martins, R.L. Reis, A.R.C. Duarte, *ACS Sustainable Chemistry & Engineering* 2 (2014) 1063.
- [14] B. Tang, W. Bi, M. Tian, K.H. Row, *J. Chromatogr. B* 904 (2012) 1.
- [15] P. Vidinha, N.M.T. Lourenco, C. Pinheiro, A.R. Bras, T. Carvalho, T. Santos-Silva, A. Mukhopadhyay, M.J. Romao, J. Parola, M. Dionisio, J.M.S. Cabral, C.A.M. Afonso, S. Barreiros, *Chem. Commun.* (2008) 5842.
- [16] Y. Wang, W. Hao, J. Jacquemin, P. Goodrich, M. Atilhan, M. Khraisheh, D. Rooney, J. Thompson, *Journal of Chemical & Engineering Data* 60 (2015) 28.
- [17] A.R.C. Duarte, S.S. Silva, J.F. Mano, R.L. Reis, *Green Chemistry* 14 (2012) 1949.
- [18] K. Padaszyński, U. Domańska, *Journal of Chemical Information and Modeling* 54 (2014) 1311.
- [19] A.P. Abbott, G. Capper, D.L. Davies, R.K. Rasheed, V. Tambyrajah, *Chem. Commun.* (2003) 70.
- [20] L. Chen, M. Sharifzadeh, N. Mac Dowell, T. Welton, N. Shah, J.P. Hallett, *Green Chemistry* 16 (2014) 3098.
- [21] Q. Zhang, K. De Oliveira Vigier, S. Royer, F. Jerome, *Chem. Soc. Rev.* 41 (2012) 7108.
- [22] D. Carriazo, M.C. Serrano, M.C. Gutierrez, M.L. Ferrer, F. del Monte, *Chem. Soc. Rev.* 41 (2012) 4996.
- [23] D.V. Wagle, H. Zhao, G.A. Baker, *Acc. Chem. Res.* 47 (2014) 2299.
- [24] A.P. Abbott, J. Collins, I. Dalrymple, R.C. Harris, R. Mistry, F. Qiu, J. Scheirer, W.R. Wise, *Aust. J. Chem.* 62 (2009) 341.
- [25] S. Gore, S. Baskaran, B. Koenig, *Green Chemistry* 13 (2011) 1009.
- [26] F. Ilgen, B. Konig, *Green Chemistry* 11 (2009) 848.
- [27] G. Imperato, E. Eibler, J. Niedermaier, B. Konig, *Chem. Commun.* (2005) 1170.
- [28] Ru, B. Konig, *Green Chemistry* 14 (2012) 2969.
- [29] M. Figueiredo, C. Gomes, R. Costa, A. Martins, C.M. Pereira, F. Silva, *Electrochim. Acta* 54 (2009) 2630.
- [30] H.-R. Jhong, D.S.-H. Wong, C.-C. Wan, Y.-Y. Wang, T.-C. Wei, *Electrochim. Commun.* 11 (2009) 209.
- [31] C.A. Nkuku, R.J. LeSuer, *The Journal of Physical Chemistry B* 111 (2007) 13271.

- [32] R.J. Davey, J. Garside, A.M. Hilton, D. McEwan, J.W. Morrison, *Nature* 375 (1995) 664.
- [33] I. Gill, E. Vulfson, *Trends Biotechnol.* 12 (1994) 118.
- [34] J.T. Gorke, F. Srienc, R.J. Kazlauskas, *Chem. Commun.* (2008) 1235.
- [35] R. López-Fandiño, I. Gill, E.N. Vulfson, *Biotechnol. Bioeng.* 43 (1994) 1024.
- [36] P. Domínguez de María, Z. Maugeri, *Curr. Opin. Chem. Biol.* 15 (2011) 220.
- [37] H. Zhao, G.A. Baker, *Journal of Chemical Technology & Biotechnology* 88 (2013) 3.
- [38] M. Sharma, C. Mukesh, D. Mondal, K. Prasad, *RSC Advances* 3 (2013) 18149.
- [39] P.W. Stott, A.C. Williams, B.W. Barry, *J. Controlled Release* 50 (1998) 297.
- [40] Y.H. Choi, J. van Spronsen, Y. Dai, M. Verberne, F. Hollmann, I. W.C.E. Arends, G.-J. Witkamp, R. Verpoorte, *Plant Physiology* 156 (2011) 1701.
- [41] Y. Dai, J. van Spronsen, G.-J. Witkamp, R. Verpoorte, Y.H. Choi, *Anal. Chim. Acta* 766 (2013) 61.
- [42] K. Shahbaz, F.S. Mjalli, G. Vakili-Nezhaad, I.M. AlNashef, A. Asadov, M.M. Farid, *J. Mol. Liq.* 222 (2016) 61.
- [43] S.-H. Wu, A.R. Caparanga, R.B. Leron, M.-H. Li, *Thermochim. Acta* 544 (2012) 1.
- [44] T. Altamash, M.S. Nasser, Y. Elhamarnah, M. Magzoub, R. Ullah, B. Anaya, S. Aparicio, M. Atilhan, *ChemistrySelect* 2 (2017) 7278.
- [45] W. Wagner, A. Pruss, *J. Phys. Chem. Ref. Data* 22 (1993) 783.
- [46] T. Altamash, M. Atilhan, A. Aliyan, R. Ullah, M. Nasser, S. Aparicio, *Chemical Engineering & Technology* 40 (2017) 778.
- [47] C. Chiappe, D. Pieraccini, *J. Phys. Org. Chem.* 18 (2005) 275.
- [48] F. Karadas, B. Köz, J. Jacquemin, E. Deniz, D. Rooney, J. Thompson, C.T. Yavuz, M. Khraisheh, S. Aparicio, M. Atilhan, *Fluid Phase Equilib.* 351 (2013) 74.
- [49] D.J.G.P. van Osch, L.F. Zubeir, A. van den Bruinhorst, M.A.A. Rocha, M.C. Kroon, *Green Chemistry* 17 (2015) 4518.
- [50] E.F. Mellon, A.H. Korn, S.R. Hoover, *J. Am. Chem. Soc.* 69 (1947) 827.
- [51] R. Ullah, M. Atilhan, B. Anaya, M. Khraisheh, G. Garcia, A. ElKhattat, M. Tariq, S. Aparicio, *PCCP* 17 (2015) 20941.
- [52] R.D. ANDRADE P, R. LEMUS M, C.E. PÉREZ C, *Vitae* 18 (2011) 325.

- [53] M. Mathlouthi, B. Rogé, *Food Chem.* 82 (2003) 61.
- [54] M.S. Nasser, M.J. Al-Marri, A. Benamor, S.A. Onaizi, M. Khraisheh, M.A. Saad, *Korean Journal of Chemical Engineering* (2015) 1.
- [55] C.O. Rossi, C. Cretu, L. Ricciardi, A. Candreva, M. La Deda, I. Aiello, M. Ghedini, E.I. Szerb, *Liquid Crystals* (2016) 1.
- [56] J.-i. Horinaka, A. Okamoto, T. Takigawa, *International Journal of Biological Macromolecules* 91 (2016) 789.
- [57] M.S. Nasser, S.A. Onaizi, I.A. Hussein, M.A. Saad, M.J. Al-Marri, A. Benamor, *Colloids and Surfaces A: Physicochemical and Engineering Aspects* 507 (2016) 141.
- [58] W. Al-Sadat, M. Nasser, F. Chang, H. Nasr-El-Din, I. Hussein, *Journal of Petroleum Science and Engineering* 122 (2014) 458.
- [59] A. Basaiahgari, S. Panda, R.L. Gardas, *Fluid Phase Equilibria* 448 (2017) 41.
- [60] M. Nasser, A. James, *Colloids and Surfaces A: Physicochemical and Engineering Aspects* 301 (2007) 311.
- [61] M.S. Nasser, A.E. James, *Colloids and Surfaces A: Physicochemical and Engineering Aspects* 315 (2008) 165.
- [62] J.D. Ferry, *Viscoelastic Properties of Polymers*. third edition edn. John Wiley & Sons, New York, 1980.
- [63] W. Al-Sadat, M. Nasser, F. Chang, H. Nasr-El-Din, I. Hussein, *Journal of Petroleum Science and Engineering* 124 (2014) 341.
- [64] J.J. Cooper-White, R.C. Crooks, D.V. Boger, *Colloids and Surfaces A: Physicochemical and Engineering Aspects* 210 (2002) 105.
- [65] L.E. Rodd, J.J. Cooper-White, D.V. Boger, G.H. McKinley, *Journal of Non-Newtonian Fluid Mechanics* 143 (2007) 170.
- [66] L.E. Rodd, T.P. Scott, D.V. Boger, J.J. Cooper-White, G.H. McKinley, *Journal of Non-Newtonian Fluid Mechanics* 129 (2005) 1.

**List of Tables**

**Table 1.** Properties of studied NADES samples in this work.

**List of Figures**

**Figure 1.** Picture of the studied NADES samples in this work.

**Figure 2.** Density values of Be:La, Be:Ma, Al:La, Al:Ma and comparison with previously studied NADES and DES systems[46, 51] (Paa=Phynlacetic acid, Laa=levulinic acid, ChCl=choline chloride, Fr=fructose)

**Figure 3.** TGA analysis for Be:La, Be:Ma, Al:LA and Al:MA NADES systems.

**Figure 4.** FTIR analysis for Be:La, Be:Ma, Al:LA and Al:MA NADES systems.

**Figure 5.** Gas sorption in Be:La NADES system at different isotherms; (a) CO<sub>2</sub> (b) N<sub>2</sub> (closed symbols are absorption and open symbols are desorption)

**Figure 6.** Gas sorption in Be:Ma NADES system at different isotherms; (a) CO<sub>2</sub> (b) N<sub>2</sub> (closed symbols are absorption and open symbols are desorption)

**Figure 7.** Gas sorption in Al:La NADES system at different isotherms; (a) CO<sub>2</sub> (b) N<sub>2</sub> (closed symbols are absorption and open symbols are desorption)

**Figure 8.** Gas sorption in Al:Ma NADES system at different isotherms; (a) CO<sub>2</sub> (b) N<sub>2</sub> (closed symbols are absorption and open symbols are desorption)

**Figure 9.** Maximum gas sorption in studied NADES systems.

**Figure 10.** Dynamic Strain Sweep used to derive the linear viscoelastic range for Be: LA and Al:La samples at a constant frequency of 5 rad/sec and at 25°C.

**Figure 11.** Effect of heating on the apparent viscosity (at low shear rate of 1 s<sup>-1</sup>) for studied NADES systems

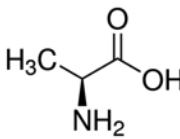
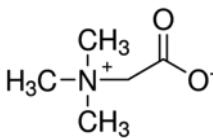
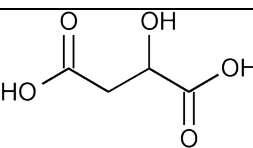
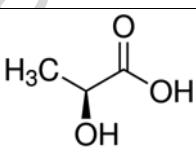
**Figure 12.** The variation of yield stress as a function of the temperature for the studied NADES systems

**Figure 13.** The variation of yield stress as a function of the angular frequency for the studied NADES systems

**Figure 14.** The variation of (a) Storage modulus (G'), (b) loss modulus (G'') and (c) complex viscosity ( $\eta^*$ ) for the NADES systems with temperature at constant frequency of 1 rad/s

**Figure 15.** Effect of heating (Ramp up) and cooling (Ramp down) on the apparent viscosity (at low shear rate of 1 s<sup>-1</sup>) for (a) Be:La and (b) Al:La NADES systems

**Table 1.** Properties of studied NADES samples in this work.

| NADES Sample   | [Al]:[Ma]   | [Be]:[Ma] | [Al]:[La]   | [Be]:[La] |
|--|---|-----------|---|-----------|
| <b>Hydrogen Bond Acceptors (HBA)</b>                           |  |           |  |           |
|  | Alanine   |           | Betaine   |           |
| <b>Hydrogen Bond Donors (HBD)</b>                              |  |           |  |           |
|  | Malic Acid  |           | Lactic Acid   |           |
| <b>Molar Mixing Ratio</b>                                      | 1:1   | 1:1       | 1:1   | 1:1       |
| <b>Liquid at [°C]</b>  | 45  | 45        | 25  | 25        |
| <b>Experimental Density<sup>a,b,c</sup> [kg/m<sup>3</sup>]</b> | 1.400   | 1.300     | 1.269   | 1.195     |
| <b>Water Content [ppm]</b>                                     | 53,972  | 27,386    | 44,417  | 7,631     |
| <b>Water Content [%]</b>                                       | 5.4%  | 2.7%      | 4.4%  | 0.7%      |

<sup>a</sup> Experimental density value at 45 °C

<sup>b</sup> Standard uncertainties  $u$  are  $u_r(\text{density}) = 0.003$  and  $u(\text{temperature}) = 0.05$  K

<sup>c</sup> Densities are reported at 0.1 MPa

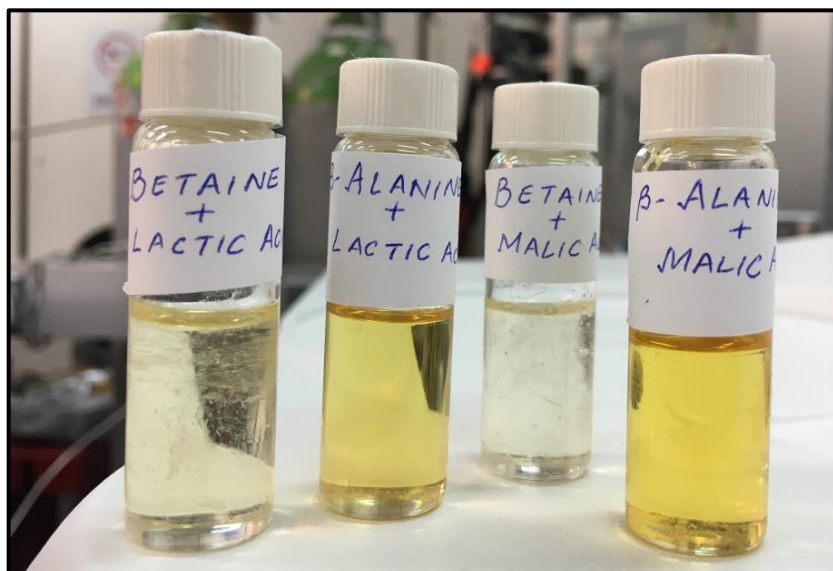


**Figure 1.** Picture of the studied NADES samples in this work.



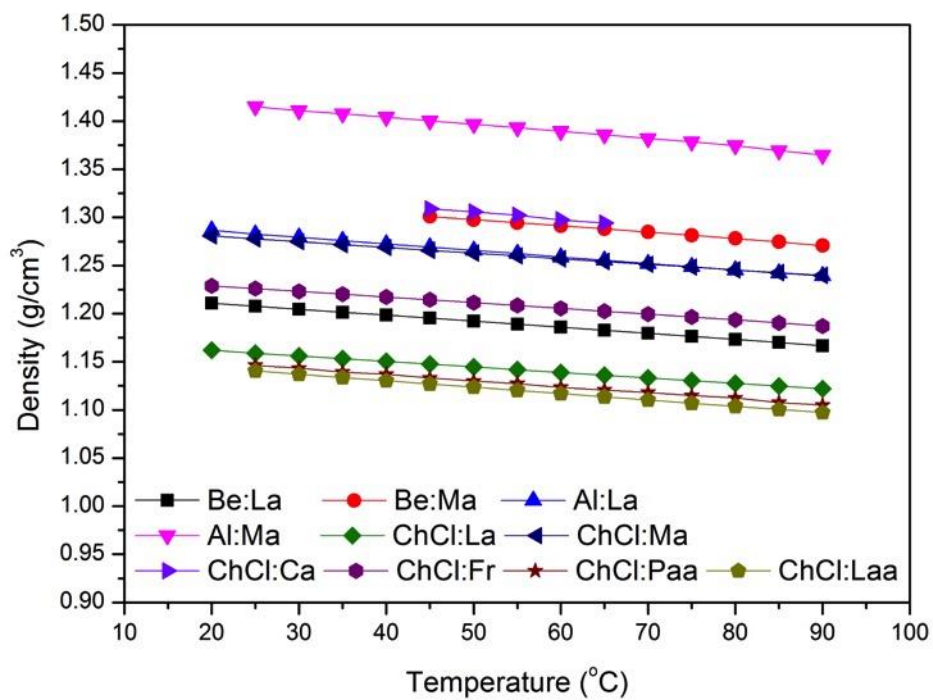


**Figure 2.** Density values of Be:La, Be:Ma, Al:La, Al:Ma and comparison with previously studied NADES and DES systems.

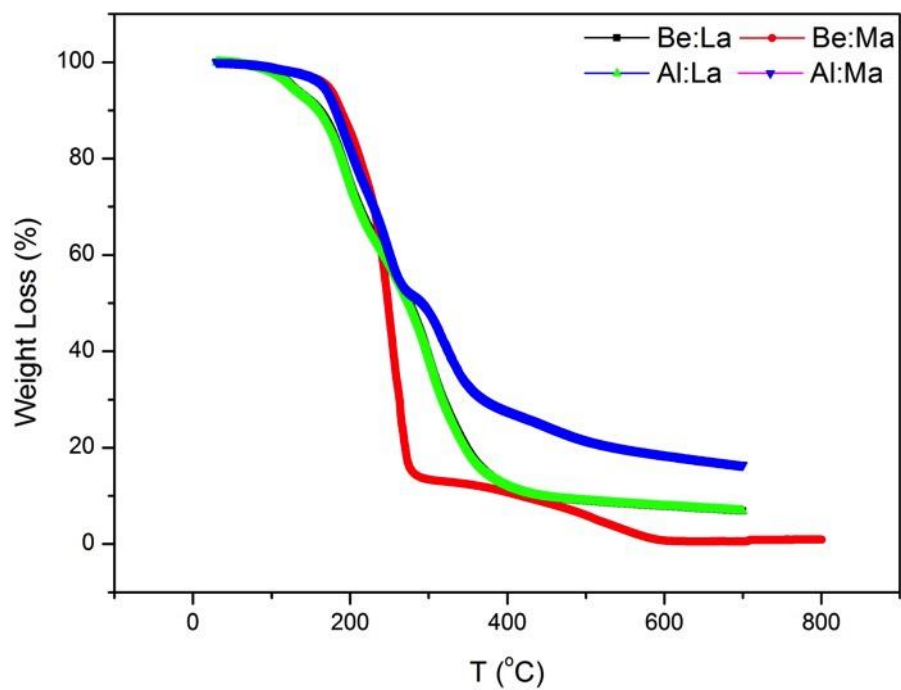


**Figure 3.** TGA analysis for Be:La, Be:Ma, Al:LA and Al:MA NADES systems.

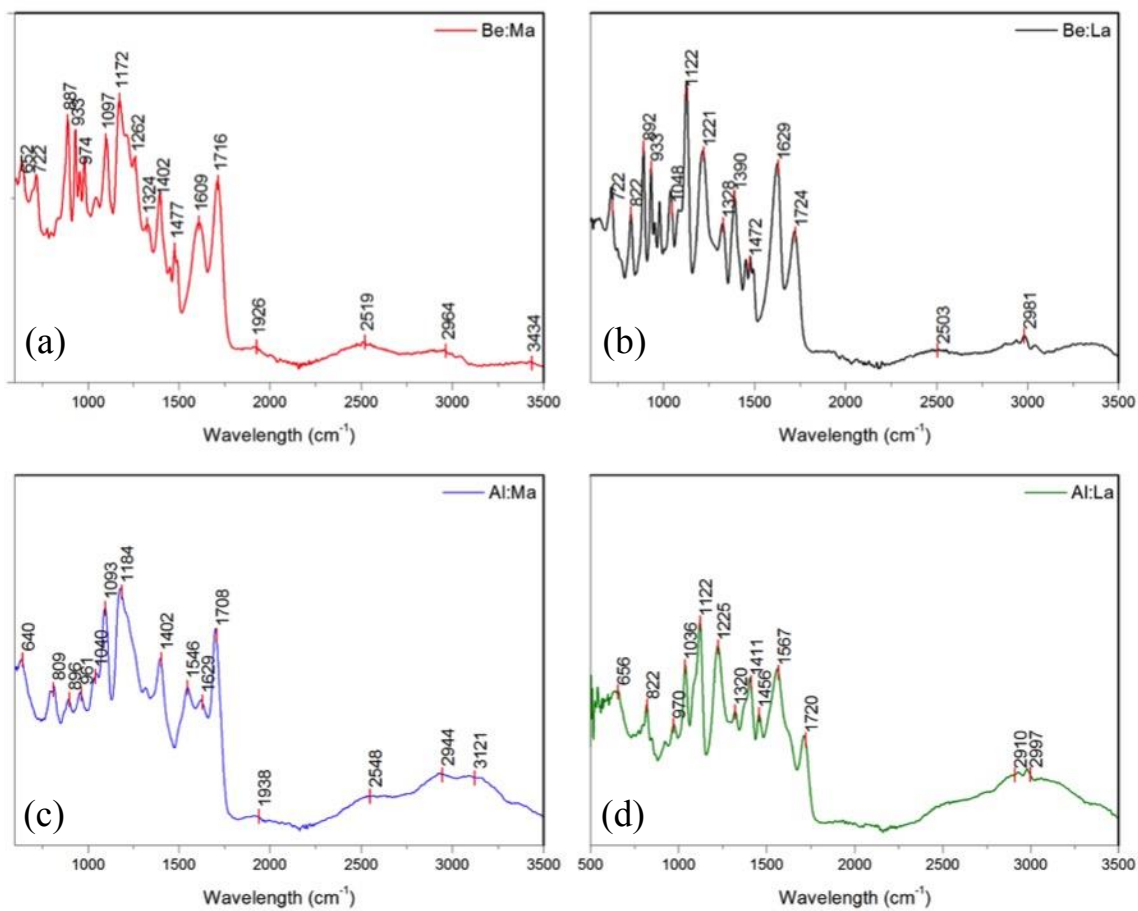


**Figure 4.** FTIR analysis for; (a) Be:La, (b) Be:Ma, (c) Al:LA and (d) Al:MA NADES systems.

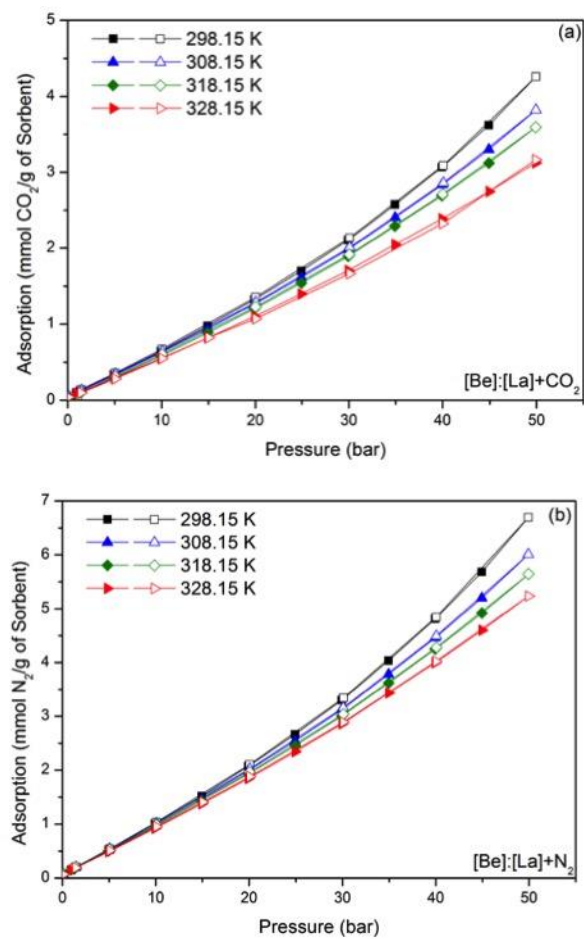


**Figure 5.** Gas sorption in Be:La NADES system at different isotherms; (a) CO<sub>2</sub> (b) N<sub>2</sub>  
(closed symbols are absorption and open symbols are desorption)

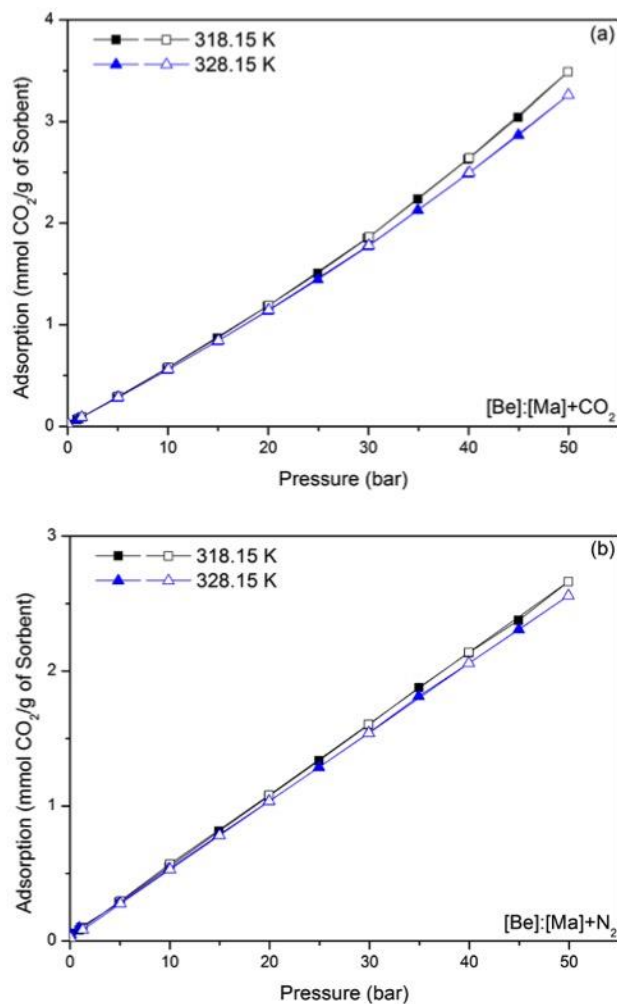


**Figure 6.** Gas sorption in Be:Ma NADES system at different isotherms; (a) CO<sub>2</sub> (b) N<sub>2</sub> (closed symbols are absorption and open symbols are desorption)

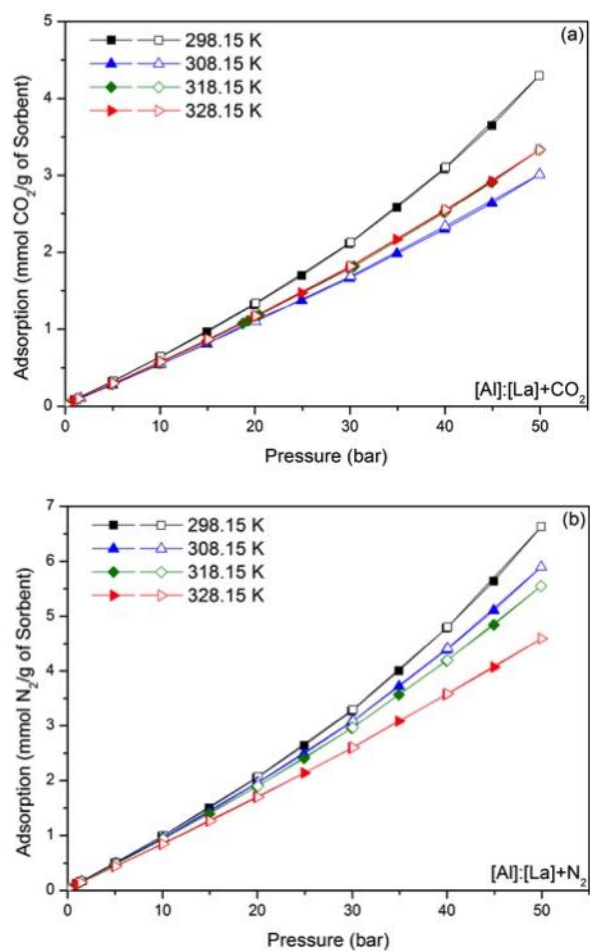


**Figure 7.** Gas sorption in Al:La NADES system at different isotherms; (a) CO<sub>2</sub> (b) N<sub>2</sub> (closed symbols are absorption and open symbols are desorption)

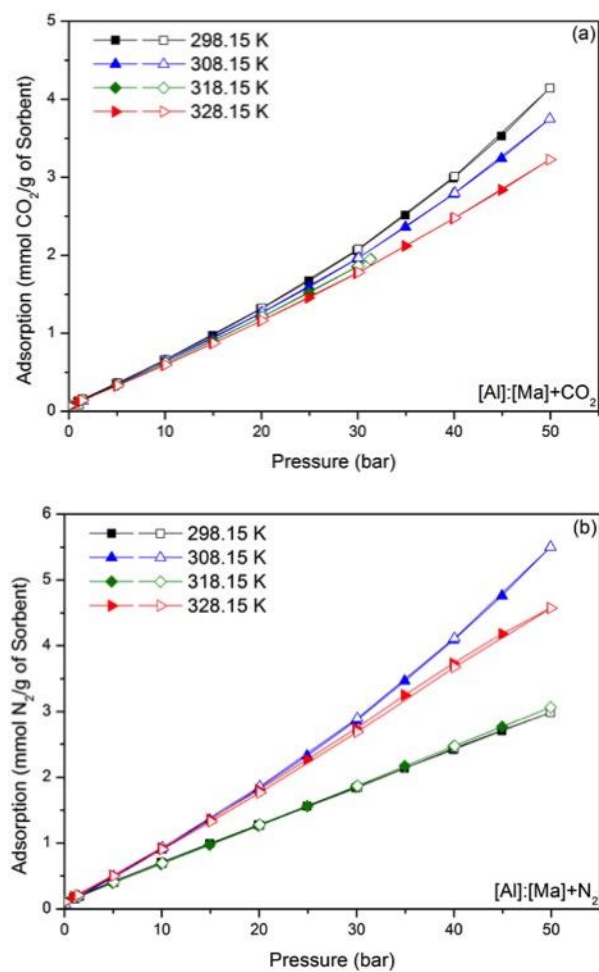


**Figure 8.** Gas sorption in Al:Ma NADES system at different isotherms; (a) CO<sub>2</sub> (b) N<sub>2</sub> (closed symbols are absorption and open symbols are desorption)

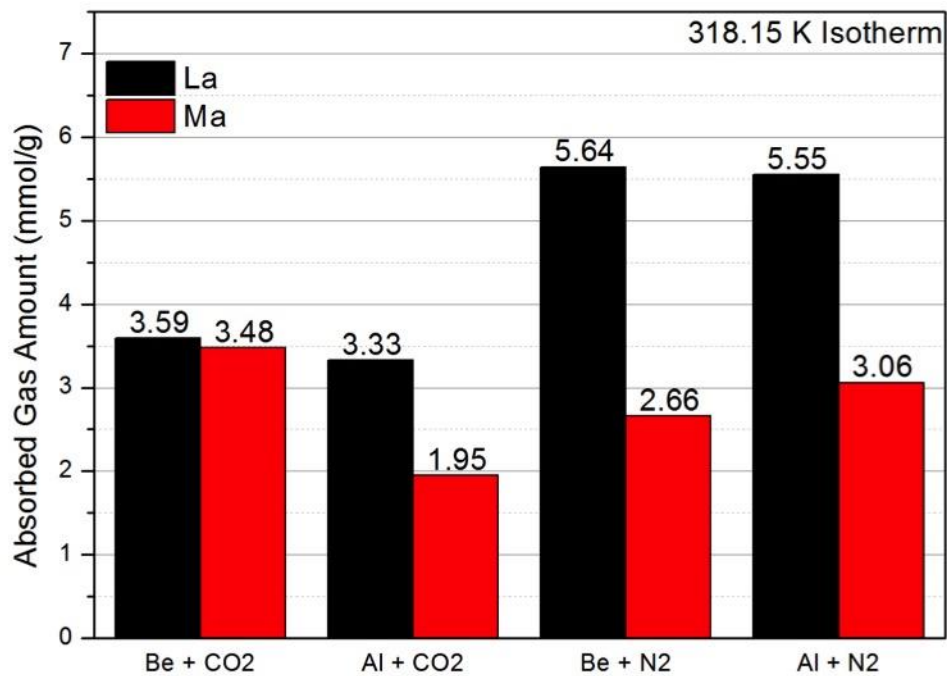


**Figure 9.** Maximum gas sorption in studied NADES systems.



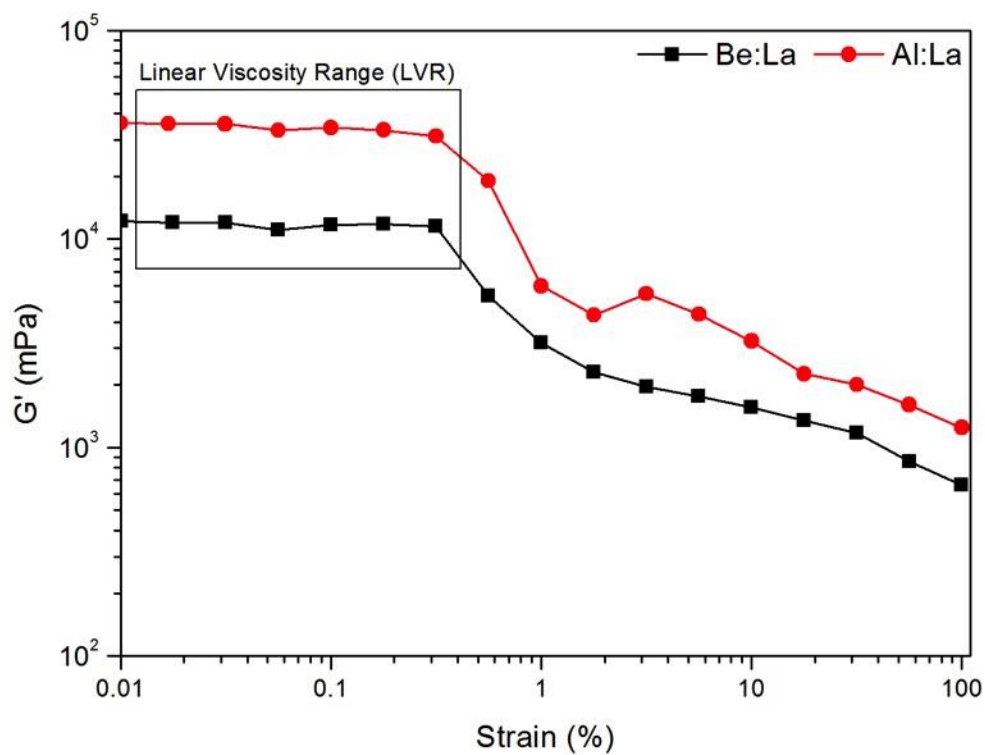


**Figure 10.** Dynamic Strain Sweep used to derive the linear viscoelastic range for Be: LA and Al:La samples at a constant frequency of 5 rad/sec and at 25°C.

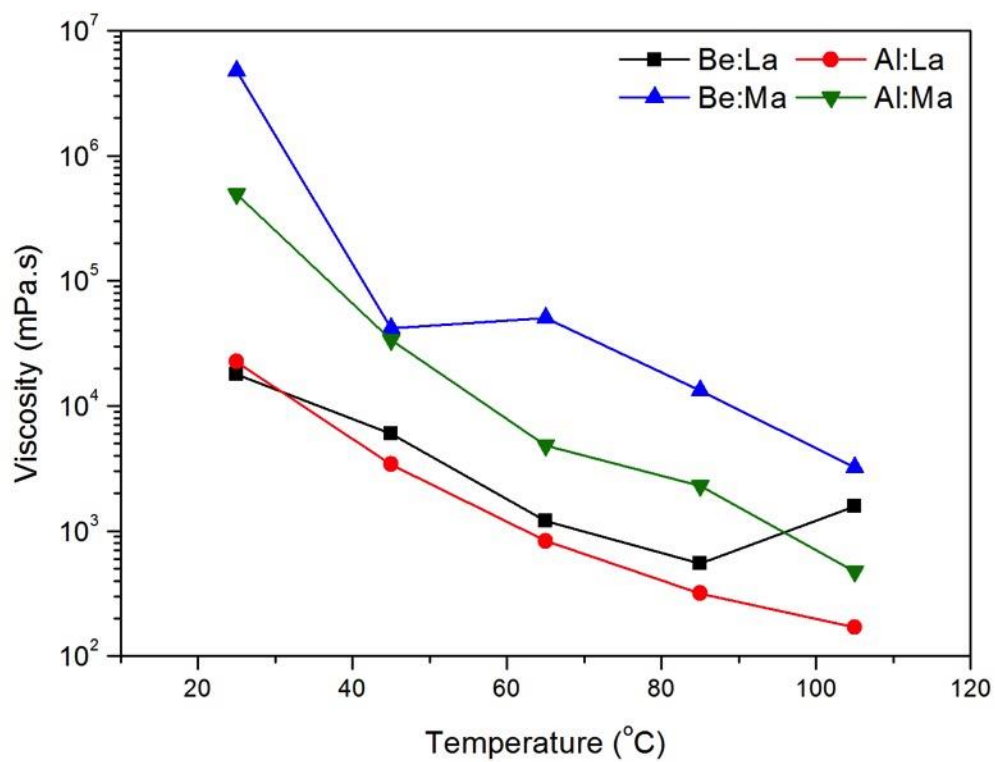


**Figure 11.** Effect of heating on the apparent viscosity (at low shear rate of  $1 \text{ s}^{-1}$ ) for studied NADES systems

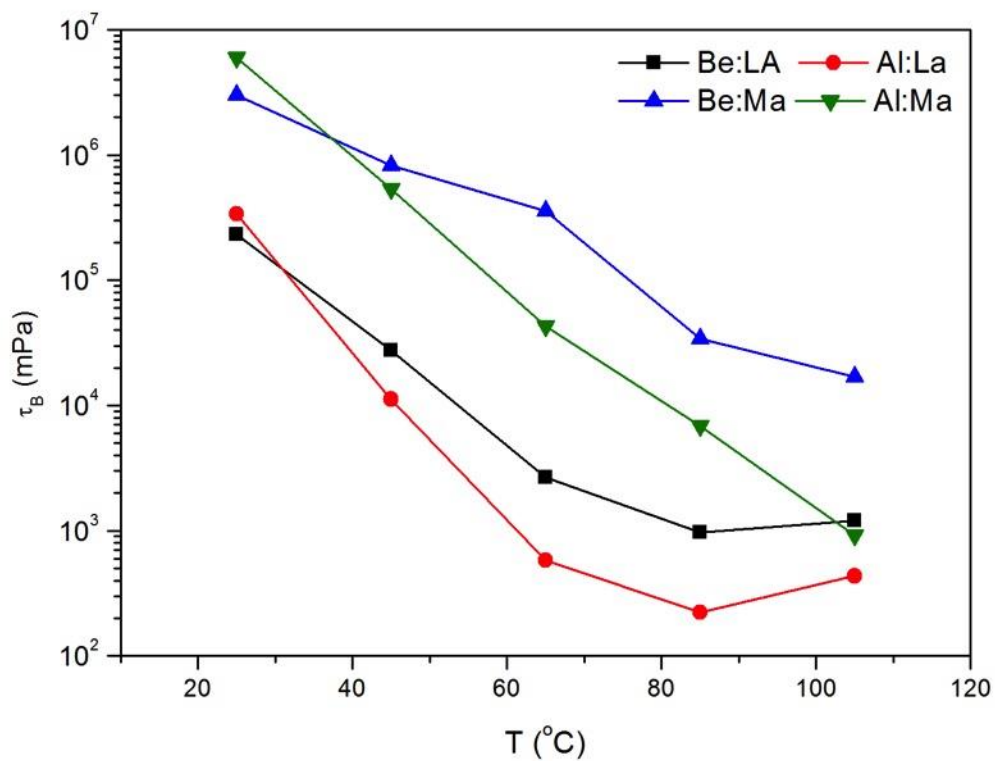


**Figure 12.** The variation of yield stress as a function of the temperature for the studied NADES systems

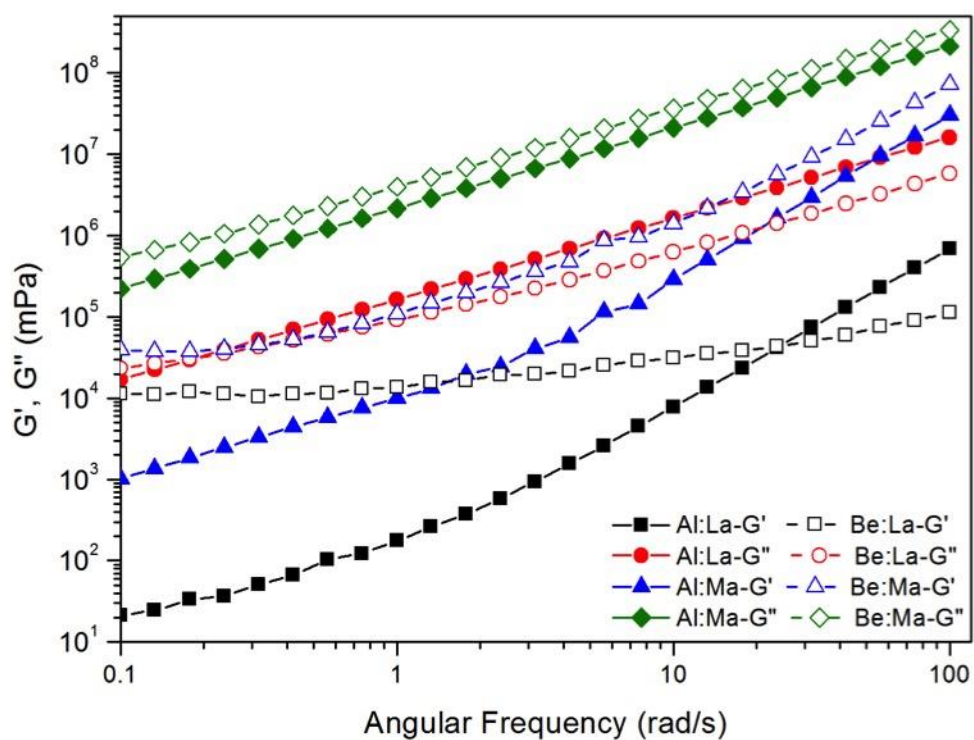


**Figure 13.** The variation of yield stress as a function of the angular frequency for the studied NADES systems

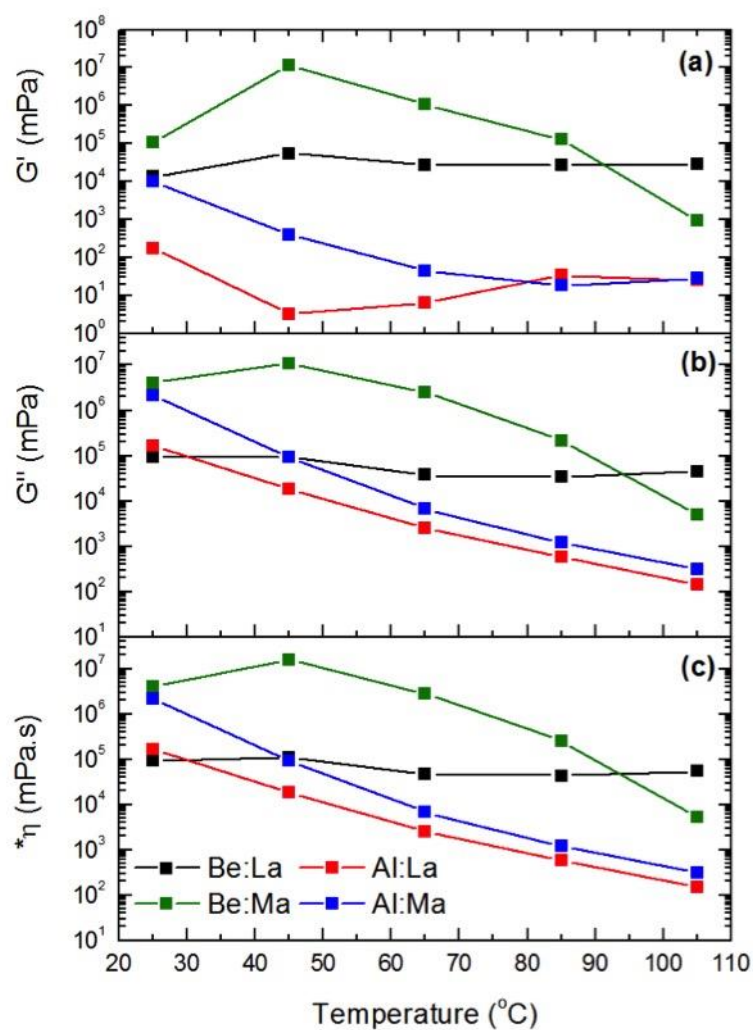


**Figure 14.** The variation of (a) Storage modulus ( $G'$ ), (b) loss modulus ( $G''$ ) and (c) complex viscosity ( $\eta^*$ ) for the NADES systems with temperature at constant frequency of 1 rad/s

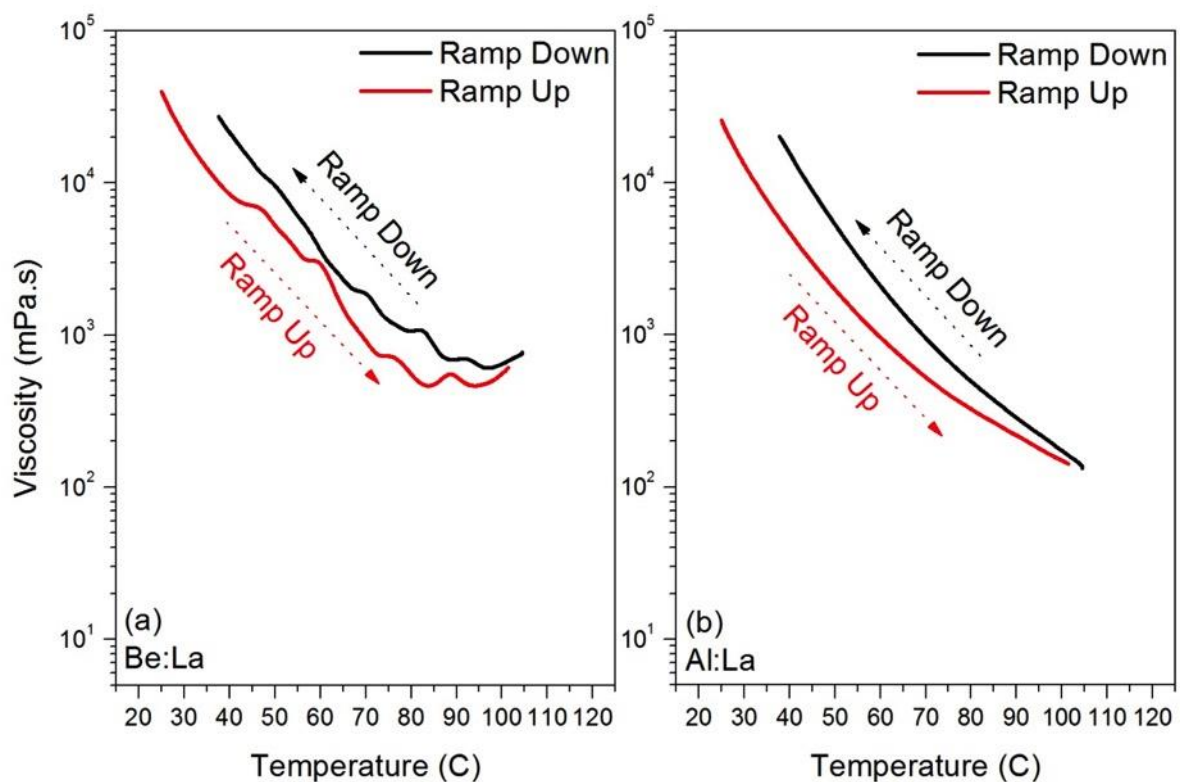
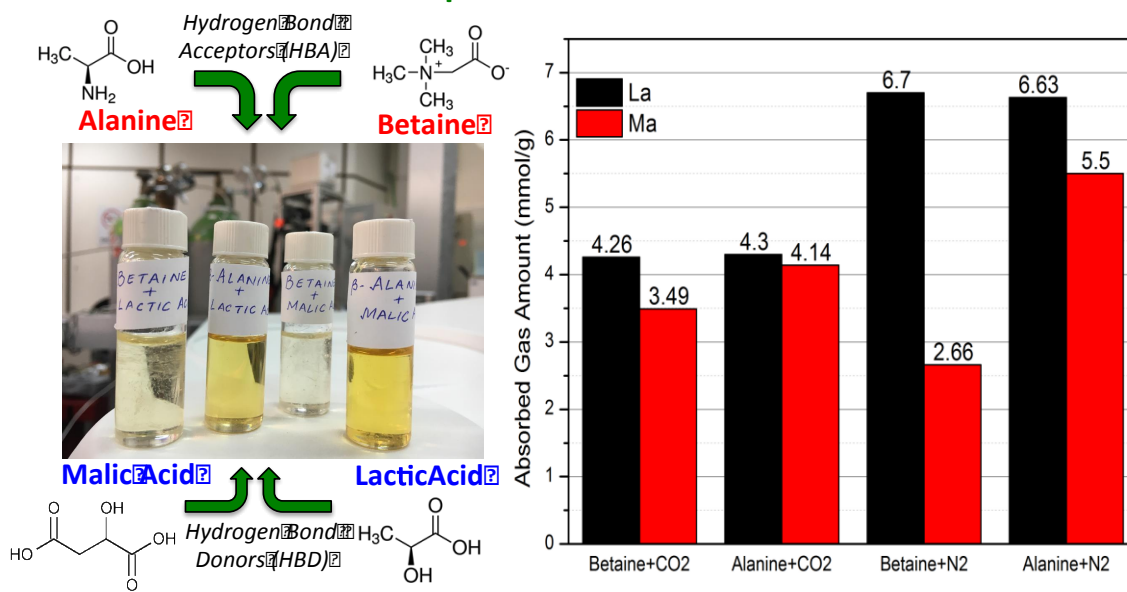


**Figure 15.** Effect of heating (Ramp up) and cooling (Ramp down) on the apparent viscosity (at low shear rate of  $1 \text{ s}^{-1}$ ) for (a) Be:La and (b) Al:La NADES systems

## Natural Deep Eutectic Solvents (NADES)



GRAPHICAL ABSTRACT

**Highlights.**

- Deep eutectic solvents prepared by using natural products.
- Enhanced CO<sub>2</sub> solubility in low toxic gas absorbents.
- Effect of yield stress, shear rate and hear on NADES rheological properties.

ACCEPTED MANUSCRIPT